AN EXPERIMENTAL STUDY AND SIMULATION WITH FLUENT OF THE HORIZONTAL–AXIS WIND TURBINE (HAWT) BLADE–TOWER DYNAMIC INTERACTION

V. P. CAMBANIS[1] & H. STAPOUNTZIS[2]
Lab. of Fluid Mechanics & Turbomachinery, Dept. of Mechanical & Industrial Enrg.,
Univ. of Thessaly, Pedion Areos, 38334 Volos, Greece
Tel.: +30 421 74109, Fax: +30 421 74052
[1]E–mail: cambanis@mie.uth.gr [2]E–mail: erikos@mie.uth.gr

ABSTRACT
The influence of the blade passage in the vicinity of a HAWT tower is investigated numerically with FLUENT and experimentally in wind tunnel. Attention is focused in the velocity and unsteady pressure fields Around the blade. For simplicity the flip type 2–D case is considered, where the blade (2–D wing with NACA 63 215 profile) is stationary while the tower (a circular cylinder) is rotated. The conditionally averaged magnitudes of wake velocities and blade lifts are in good agreement with those calculated by FLUENT. It is also encouraging that the phase positions of the experimental velocity and lift overshoot correspond to the calculated ones.

1. INTRODUCTION AND SCOPE

The problem considered in this study is the unsteady loading of a wind turbine blade, which is exposed to the wake of a cylindrical pylon located upstream. Of prime interest is the effect of proximity of the blade to the bluff body. FLUENT5.5 was used for the numerical simulation and a wind tunnel for the experiments. It was much more convenient to set up the reverse experiment, namely that of a rotating 2–D cylinder and a stationary 2–D airfoil, as shown in Fig. 1. Results are presented for zero angle of incidence of the airfoil.

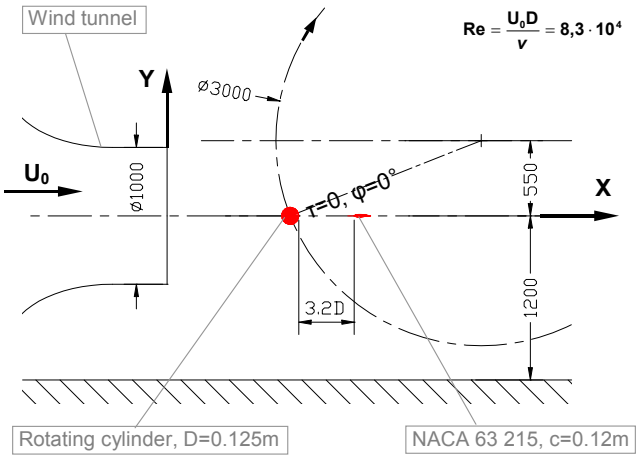

Figure 1: Schematic of Experimental Set–up and Numerical Simulation.

As far as the authors are aware, the problem of current investigation attracted attention quite recently and therefore has not been well documented in the literature. The experimental results given in section 3, stem from the contribution of the present research group to the European Community Joule Project [1]. Earlier work [2] that dealt with the static counterpart has shown that the presence of the cylinder causes an overall decrease in the surface pressure distribution mainly in the leading edge region. The lift coefficient and its slope are lowered

depending on the transverse position of the cylinder with respect to the airfoil. The airfoil near wake is dominated by the cylinder wake, which is slowly decaying. The influence of homogeneous spanwise shear on the airfoil wake is to smooth out the velocity deficit caused by the cylinder. The results are in conformity with those of [3] and [4]. Large–scale vortex development is prevented by the intrusion of the leading edge of the plate in the near wake region. However, unstable disturbances are maintained in the shear layers separating from the cylinder. For a cylinder and a plate of comparable size, a streamwise gap of about 4 cylinder diameters seems to cause the most significant reduction in regular von Kármán shedding.

It is known that the modification of the vortical wake and the suppression of vortex shedding by an airfoil (or splitter plate) are due to the inability of the separated shear layers to come close together and mix their vorticities. The question posed in this work is to which extent the flow periodicity due to the cylinder rotation affects the wake and the dynamic loading of the blade.

2. NUMERICAL COMPUTATIONS WITH FLUENT

FLUENT5.5.14 commercial CFD code was used to solve numerically the 2–D problem for the same geometry and flow conditions as in the experiment. The model that was designed in GAMBIT1.3 pre–processor with the boundary conditions is shown in Fig. 2. The main grid was unstructured with triangular mesh elements. In the vicinity of the airfoil and the cylinder a structured grid of quadrilateral mesh elements (boundary layer capability) was created.

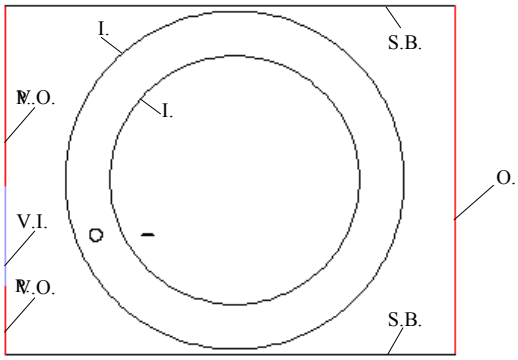

Figure 2: Boundary Conditions (V.I., Velocity Inlet; P.O., Pressure Outlet; O., Outflow; S.B., Solid Boundary/Wall and I., Interface).

In Figs. 3 and 4 this boundary–layer grid for the cylinder and the airfoil is shown. In order to control the size of the unstructured grid several auxiliary internal surfaces were created. Due to the dynamic nature of the problem separate areas with sliding and static meshes were required and constructed and TFilter2.5 was used to connect them. The final grid after the connection and the reordering procedure sized approximately 29000 nodes. The solution is time–dependent, which means that the unsteady version was used. The case was solved with the segregated solver and the sliding mesh capability. The turbulence model that was applied was the standard k–ε keeping the parameters to the default values (C_μ=0.09, $C_{1\varepsilon}$=1.44, $C_{2\varepsilon}$=1.92, σ_k=1.0, σ_ε=1.3.) After initial testing, with the aim to achieve convergence, it was found that the under–relaxation factors should take the following values: pressure→0.3, momentum→0.5, k→0.5, and ε→0.5. Also the discretization schemes for the convection terms of each governing equation should kept to the default value. Several attempts were done –without convergence to be achieved– by using combinations of the following parameters for the descretization scheme: body forced for pressure, 2nd order for moment and PISO for pressure–velocity coupling. The time step was chosen to be 10^{-3}T, so that period would be composed by a sufficient number of steps (1000).

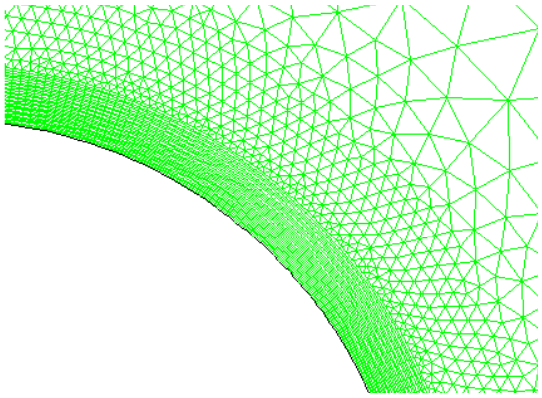

Figure 3: Near–Cylinder Mesh.

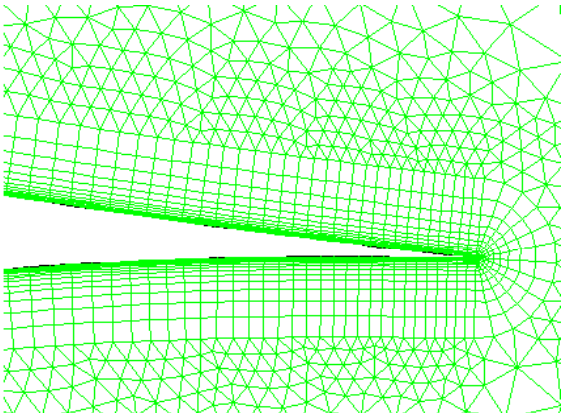

Figure 4: Near–Airfoil Mesh.

Results of such computations are given bellow for the following cases:

a. static cylinder and airfoil,
b. dynamic cylinder only and
c. full case (dynamic cylinder and airfoil).

The problem that is studied is unsteady. Even when the cylinder is not moving (static) the shedding vorticity is an unsteady process. In order to have a guess of the initial conditions and to reduce the computational effort the problem was solved in all cases with the steady formulation. The solution that was achieved was used to initialise the flow field and then it was solved taking into account the time dependency.

a). The first case studied with FLUENT is the static problem (static cylinder–static airfoil). A snapshot of the vorticity contours is illustrated in Fig. 5, while Fig. 6 is the respective case without the blade. Studying the sequence of vorticity contour images (animation), it can be noticed that the presence of the blade leads to a steady vorticity pattern, which was not expected and that is under investigation.

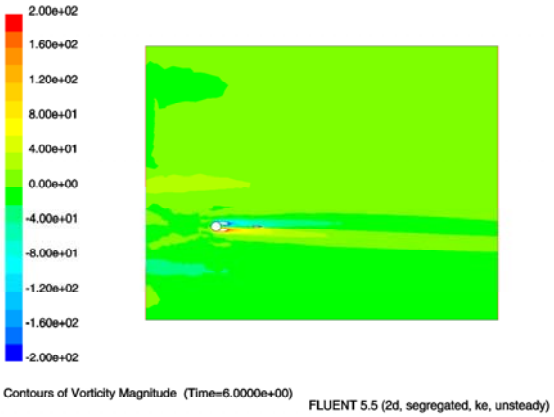

Figure 5: Vorticity Contours for Static Cylinder and Airfoil at $\alpha=0^o$.

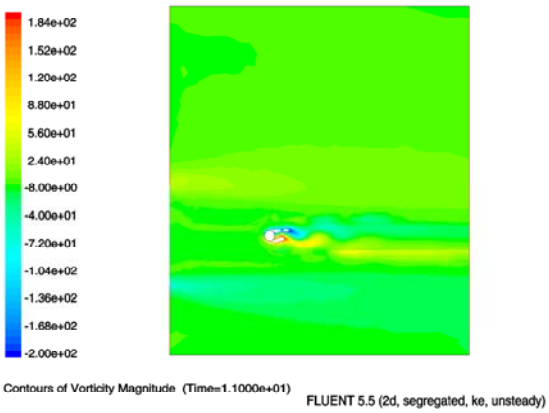

Figure 6: Vorticity Contours; Cylinder Only.

b). The next case concerns the dynamic cylinder configuration. Velocity and vorticity contours are shown in Figs 7 and 8. It is indicated that the wake of the cylinder (velocity deficit) causes the trough value. The entrance of the cylinder in the flow is also indicated with a crest value in axial velocity U. In Fig. 9 the axial velocity time series over one period are shown. Note that λ_o=(linear cylinder velocity magnitude)/(free stream velocity). The passage of the cylinder is indicated by several peak values. A comprehensive analysis is given in section 3.

c). The full problem (dynamic cylinder–static airfoil) is described next. As indicated in Fig. 10, the airfoil acts as a physical obstacle keeping the velocity magnitude low. Regarding vorticity contours, Fig. 11, is noticed that there are high levels of vorticity shed from the airfoil, while the cylinder approaches it. Velocity time series, Fig. 12, are indicating higher peak values when the cylinder approaches the airfoil level. Further discussion cannot be conducted while the computational analysis is in the preliminary stage.

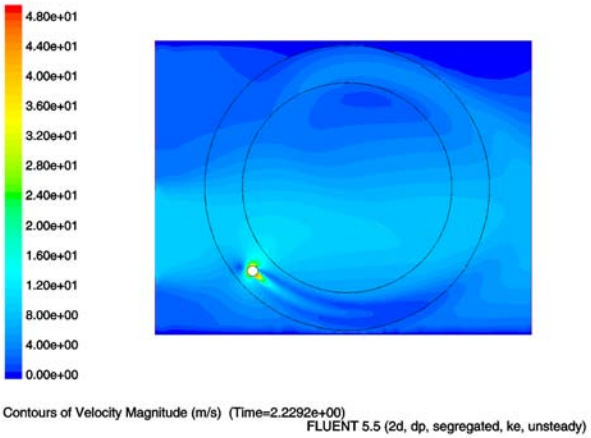

Figure 7: Velocity Contours; (Dynamic Cylinder Case).

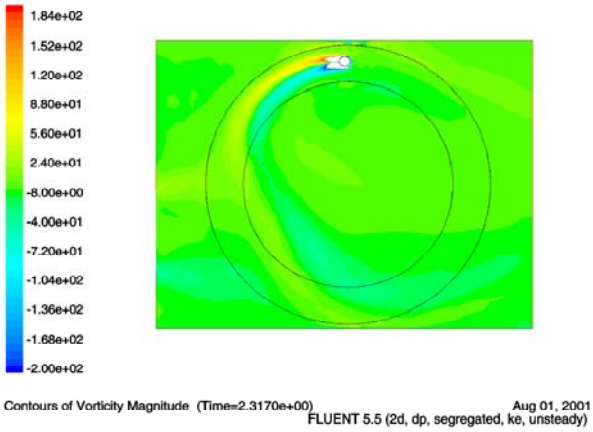

Figure 8. Vorticity Contours; (Dynamic Cylinder Case).

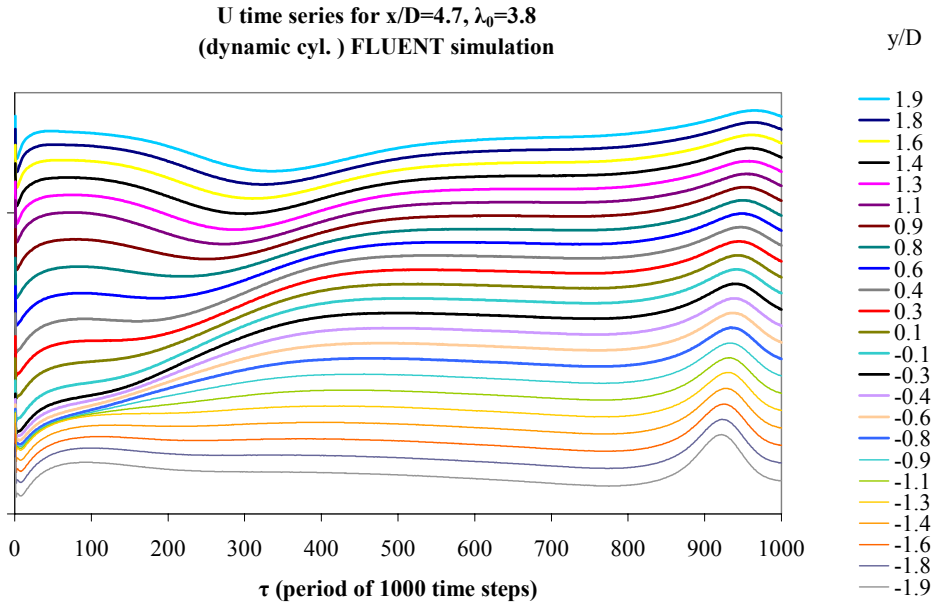

Figure 9: Velocity Time Series by FLUENT Simulation (Dynamic Cylinder Case).

The unsteady lift coefficient time record is illustrated in Fig. 13. It was computed enabling *Force Monitors* panel under *Solve* menu. As indicated, the dynamic cylinder effect is expressed as a strong negative peak of the unsteady force acting to the blade. It is noteworthy that the minimum value (approximately –2.4) is reached 13 degrees before the cylinder reaches again the airfoil plane ($\tau \cong 950$). This means that the airfoil sensed the vortical wake of the moving cylinder, while the early mild increase in the lift coefficient ($\tau \cong 30$) is probably a potential flow effect.

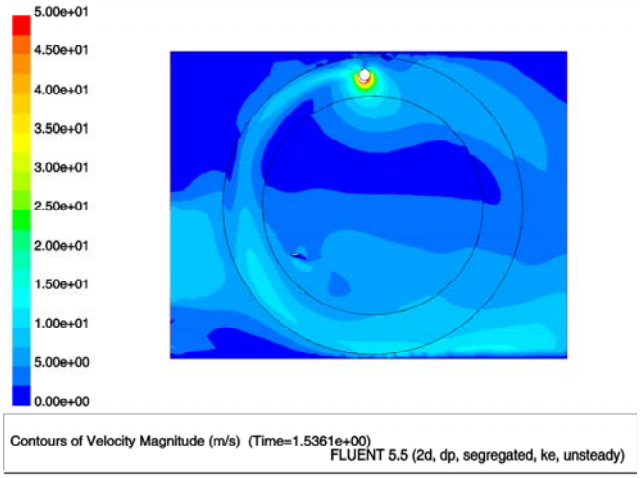

Figure10: Velocity Contours (Full Case).

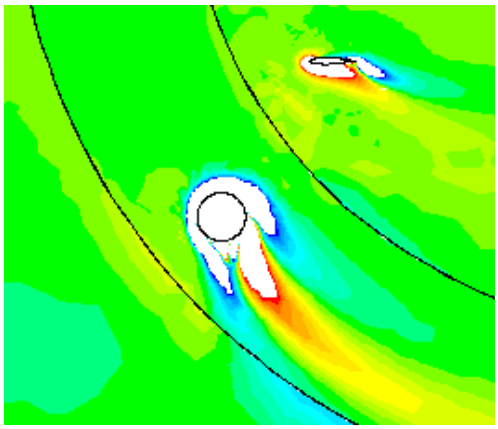

Figure 11: Detail of Vorticity Contours (Full Case).

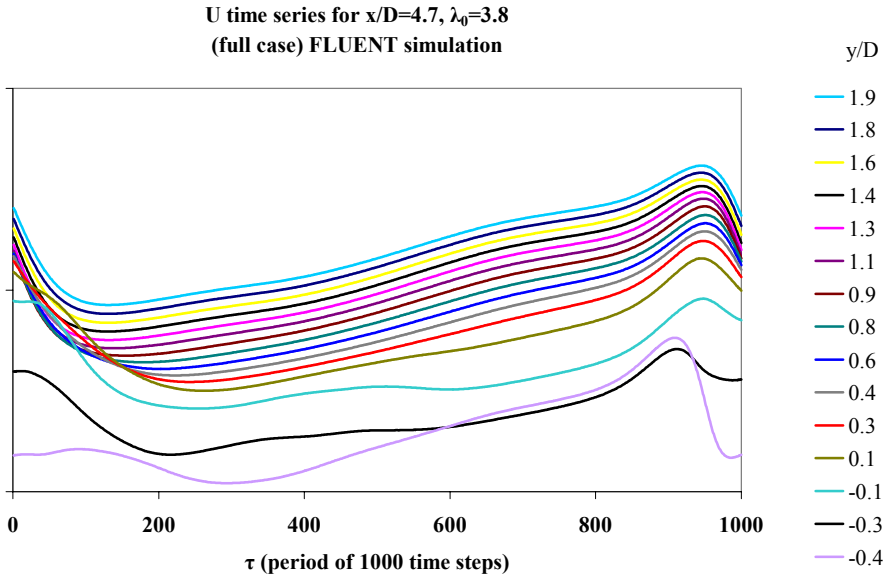

Figure 12: Velocity Time Series by FLUENT Simulation (Full Case).

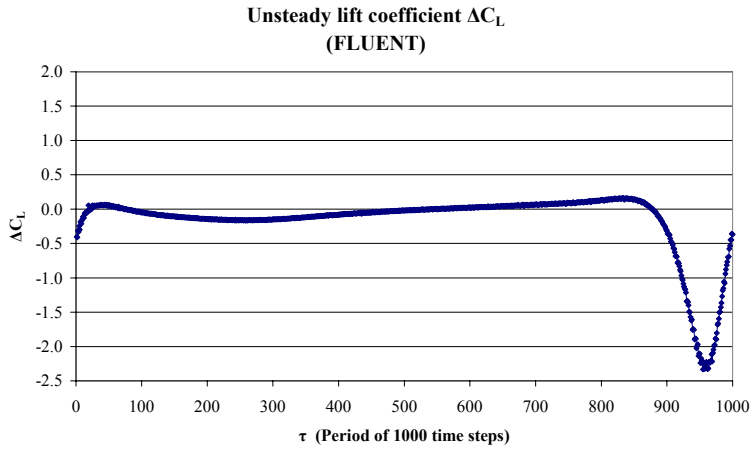

Figure 13: Unsteady Lift Coefficient by FLUENT.

3. COMPARISON WITH EXPERIMENTAL RESULTS

The measured raw data were processed to yield representative mean time–series. The results presented are therefore ensemble averaged over one period, T, of cylinder rotation. In order to investigate the complex cylinder wake itself, velocity measurements were first carried out without the presence of the airfoil.

In Fig. 14 the superimposed velocity time series (dynamic cylinder case) in position x=4.7D for 17 vertical positions are shown. The period T (one rotation) consists of 144 measurement points (τ) and lasts 0.24 s approximately.

It is possible to distinguish several peak values (crest and trough) that travel in time from one position to another. Considering these curves one may notice two types of shapes for the high and low vertical positions. These two types are sketched in Fig. 15 and are given their corresponding names in crest (C) and trough (T) values.

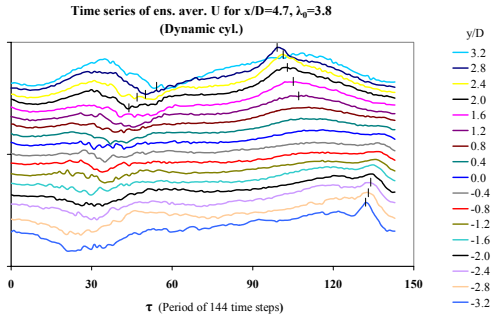

Figure 14: Ensemble–Averaged Velocity Time Series.

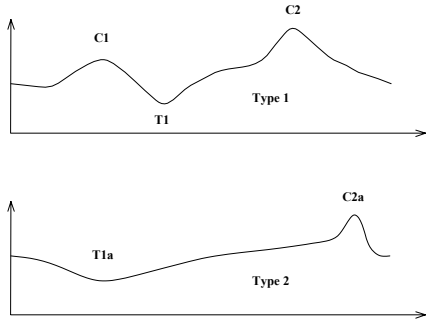

Figure 15: Characteristic Shapes of Velocity Time Series.

A shifting and merging procedure of these peak values causes the transition from the one type to the other. The location of peak values in each measuring position is determined, but only in the cases where it was clear to locate the temporal position of them. Some examples are noted in Fig. 14. This study was conducted also for the measurements in the other abscissa locations and results e.g. for T1 are summarized in Figs. 16 and 17 respectively. Peak T1 arises after the cylinder passing and the timing is consistent to the free stream velocity, which means that it indicates the existence of cylinder wake (velocity deficit).

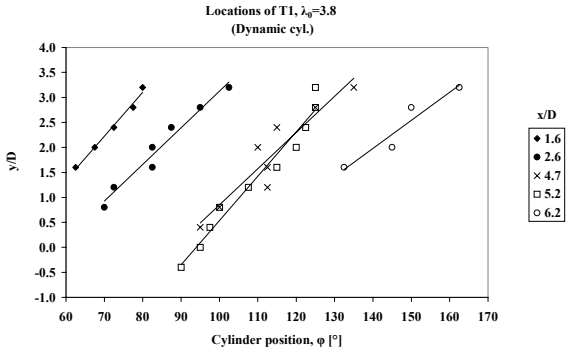

Figure 16: Temporal Locations of Peak T1.

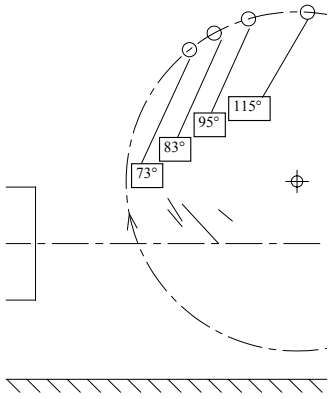

Figure 17: Locations of T1 Relative to Cylinder's Angular Position.

However the shape of experimental velocity time series is not following exactly the shape shown in Fig. 9, computed by FLUENT. Probable reasons are that computational analysis was done only for a few initial periods and also 3–D effects were neglected.

Measurements of unsteady pressure distribution led to estimation of unsteady lift coefficient. In Fig. 18 C_L during the mean period is shown. The dynamic motion of the cylinder is indicated by a trough value followed by a weaker increase, which does not agree exactly with the computational results of FLUENT, partly due to above mentioned reasons. Also, unsteady pressure measurements were conducted only in 17 positions around the airfoil, while numerically C_P is calculated in one hundred positions (Fig. 4).

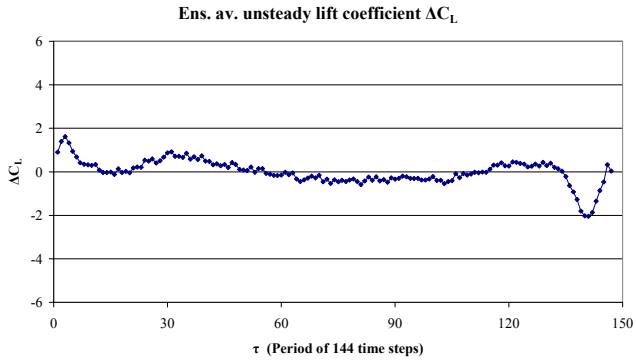

Figure 18: Experimental Lift Coefficient.

4. CONCLUSIONS

The simulation of an unsteady flow round an airfoil can be accomplished with FLUENT and its sliding mesh capability. Gross flow quantities like the wake velocity variations and the lift are in good agreement. This provides some hope that the details of the flow structure might also be well represented. It is thought that FLUENT could be employed for a systematic study of the effect of wind turbine tower–blade spacing on the dynamic loading of the latter.

REFERENCES

[1] E.U. JOULE project "ROTOW–Investigatin of the Aerodynamic Interaction Between Wind–Turbine Rotor Blades and the Tower and its Impact On Wind–Turbine Design", Final Report JOR3–CT98–0273, 1998–2000.

[2] Stapountzis H., Yakinthos K., Goulas A., Kallergis S., & Kambanis V., (1999). "Cylinder Wake–Airfoil Interaction for Application to a HAWT", *EWEC '99*, pp. 172–175, Nice, France.

[3] Anderson E., & Szewczyk A. A, (1997). "Effects of a splitter plate on the near wake of a circular cylinder in 2 and 3–dimensional flow configurations", *Exp. in Fluids*, **23(2)**, pp. 161–174.

[4] Unal M. F., & Rockwell D., (1987). "On the vortex formation from a cylinder. Part 2. Control by splitter–plate interference", *J. of Fluid Mechanics*, **90**, pp. 513–529.